frontiers | Frontiers in Environmental Science

TYPE Original Research
PUBLISHED 30 August 2022
DOI 10.3389/fenvs.2022.996353

OPEN ACCESS

EDITED BY
Wenyi Deng,
Donghua University, China

REVIEWED BY
Lili Qian,
Jiangsu University, China
Sara Fulignati,
University of Pisa, Italy

*CORRESPONDENCE
Yujie Fan,
yujie.fan@partner.kit.edu

SPECIALTY SECTION
This article was submitted to Water and Wastewater Management, a section of the journal Frontiers in Environmental Science

RECEIVED 17 July 2022
ACCEPTED 03 August 2022
PUBLISHED 30 August 2022

CITATION
Fan Y, Prestigiacomo C, Gong M, Tietz T, Hornung U and Dahmen N (2022), Comparative investigation on the value-added products obtained from continuous and batch hydrothermal liquefaction of sewage sludge. *Front. Environ. Sci.* 10:996353. doi: 10.3389/fenvs.2022.996353

Comparative investigation on the value-added products obtained from continuous and batch hydrothermal liquefaction of sewage sludge

Yujie Fan[1,2]*, Claudia Prestigiacomo[3], Miao Gong[4], Thomas Tietz[2], Ursel Hornung[2] and Nicolaus Dahmen[2]

[1]Nanyang Institute of Technology, School of Civil Engineering, Nanyang, China, [2]Karlsruhe Institute of Technology, Institute of Catalysis Research and Technology (IKFT), Karlsruhe, Germany, [3]University of Palermo, Department of Engineering, Chemical, Environmental, Biomedical, Hydraulics and Materials Section, Palermo, Italy, [4]Hefei University of Technology, School of Civil Engineering, Hefei, China

Hydrothermal liquefaction (HTL) can be considered a promising route for the energy valorisation of waste sewage sludge (SS). However, not much information is available on continuous flow processing. In this study, the mixed SS was subjected to HTL at 350°C for 8 min in a continuous reactor with loadings of 10 wt% in the feed flow. The results show that the mass recovery reached 88%, with a biocrude yield of 30.8 wt% (3.9 wt% N content). The recovered biocrude yields are highly dependent on the selection of the recovery solvent for extraction, and dichloromethane can contribute an additional 3.1 wt% biocrude from aqueous phase, acetone can extract some pyrrole derivatives into the trapped phases. Comparable results were also achieved by performing batch reactions under the same conditions: a slightly higher biocrude yield (33.1 wt%) with an N content of 4.3 wt%. The higher N content observed in the biocrude from the batch process indicates that interactions and chelation between intermediates are enhanced during heating up and cooling period, which lead to more N-containing compounds.

KEYWORDS

sewage sludge, HTL, continuous processing, biocrude, nitrogen

Introduction

The worldwide economic and social development has led to increasing output of sewage sludge (SS). Hydrothermal liquefaction (HTL) has been suggested as a cost-effective and eco-friendly solution for valorisation of SS in the field to improve waste management and contribute to the production of renewable energy carriers. Without the need for pre-drying of wet feedstock, HTL can produce liquid fuel, called biocrude, at elevated temperatures (250–370°C) and pressures (4–22 MPa), with relatively short reaction times (0–80 min) (Lin et al., 2020; Djandja et al., 2021).

In the last decades, the majority of HTL experiments have been carried out in batch reactors, typically with a few hundred millilitres of reaction volume at a time, due to their relative simplicity of operation and product collection. SS mainly comprises of water (~85–99 wt%), proteins (~40 wt%), lipids (~10–25 wt%), carbohydrates (~10 wt%), and ash (~30–50 wt %) in varying amounts depending on the source, season and pre-treatment (He et al., 2014; Gherghel et al., 2019). Owing to its volatile organic content, which is reported to be between 21 and 48 wt% in available literature, the energy of dried SS ranges from 11 to 22 MJ/kg, suggesting calorific values that are comparable to other types of biomass (Djandja et al., 2021). In addition, it is reported that compared to dry sludge, exploiting wet sludge can decrease the consumption of energy by 30% (Lu et al., 2016).

A significant advantage of a batch process is that relatively high dry matter concentrations can easily be processed as there are no complications due to difficulties in pumping the feedstocks and plugging of pipes, which frequently occur in continuous flow processes (Ali Shah et al., 2021). Collection of samples in batch HTL systems often requires relatively high amounts of solvents to extract a small amount of liquid and solid products, which is unsuitable for practical use in industrial applications and increases the uncertainty of results (Wagner et al., 2017). The attention is now increasingly shifting towards scaling up HTL processes, from lab-scale to pilot-scale plants operating with continuous flow processes.

In 1992, a Japanese group successfully tested the continuous HTL of SS with a capacity of 500 kg/d at 270–300°C and a holding time of 0–60 min, which ran for more than 700 h without any trouble (Itoh et al., 1992; Itoh et al., 1994). Organic matter in the SS was converted by 40–53 wt% into heavy oil. Elliott et al. (2015) reviewed and summarized the recent research in continuous-flow process development for biomass HTL, mostly covering algal and woody biomasses. For example, a continuous flow pilot-scale HTL process was established at the Sydney University in Australia with a reactor of approximately 2 L to liquefy micro and macro algae (Jazrawi et al., 2013; He et al., 2016). Lignocellulosic forest biomass has been tested with Hydrofraction™ technology, which was developed by Steeper Energy ApS in collaboration with Aalborg University, achieving 45.3 wt% oil yields with 85.6% energy recovery (Jensen et al., 2017).

Regarding SS, results from numerous batch experiments showed promising results for their application in continuous systems, but less information is available on pilot-scale continuous processes. Pacific Northwest National Laboratory has reported 37 wt% yields of biocrude achieved from 12 wt% dry matter slurry in a continuously stirred-stank HTL system (Marrone et al., 2018). The novel pilot-scale continuous HTL plant incorporated an oscillating flow technology, developed by Aarhus University in Denmark, and has processed algae and SS with a capacity of up to 100 L/h (Anastasakis et al., 2018; Johannsen et al., 2021). Average yields of 25 wt% biocrude was obtained by HTL of 4 wt% dry primary sludge slurry at 350°C with a 5 h retention time. However, the much lower dry content limited energy recovery to 33%, and around 20 wt% biocrude was comprised of inorganic solids owing to the separation by gravity. Biocrude produced contained 3.4 times more energy than used for HTL processing (Silva Thomsen et al., 2020).

Regarding the transfer of outputs from the lab-scale to a commercial system, the difference between batch and continuous should be considered. SS is a protein-rich waste, indicating the inevitable high amount of N-containing compounds will be converted into biocrude, which is a big challenge in terms of compliance with fuel standards (Huang et al., 2019; Rahman et al., 2021). A considerable amount of literature can be found on the investigation of nitrogen behaviour during thermal treatment of SS (Leng et al., 2020; Zimmermann et al., 2021). However, limited information is available on continuous processing. Therefore, this study aims at a comparison of the fate of N during continuous flow process operation in a bench-scale reactor with results from batch experiments.

Methodology

Materials

The SS used in the work here in, constituted by a mixing of primary and secondary sludge, was collected directly from the wastewater treatment plant in Karlsruhe, Germany. SS was stored at −18°C until used in the experiments. The frozen SS was first dewatered by freeze-drying at −82°C and a pressure of 30 mbar for 72 h (Christ Alpha 2-4 freeze-dryer), then the dried sludge was crushed in a mill (Fritsch Pulverisette 14, Germany) and filtered through a sieve (60 mesh). A certain amount of water was added to the dried sludge to achieve the designed moisture content of 90 wt%.

Deionized water was used as solvent for each HTL experimental run. Acetone, cyclohexane and dichloromethane (DCM) (Sigma-Aldrich, grade) were used as solvents to recover the produced biocrude. Tetrahydrofuran (THF) (Sigma-Aldrich, analytical grade ≥99.0%) was used as solvent to prepare samples for gas chromatographic analyses. Methyl heptadecanoate (Sigma Aldrich, analytical standard) was used as internal standard for the GC-FID analyses of the trapped phase.

HTL experimental procedure

The continuously operated HTL plant was designed and built by Karlsruhe Institute of Technology, as shown in Figure 1. It was tested to operate till a maximum temperature and pressure of 450°C and 350 bar, respectively.

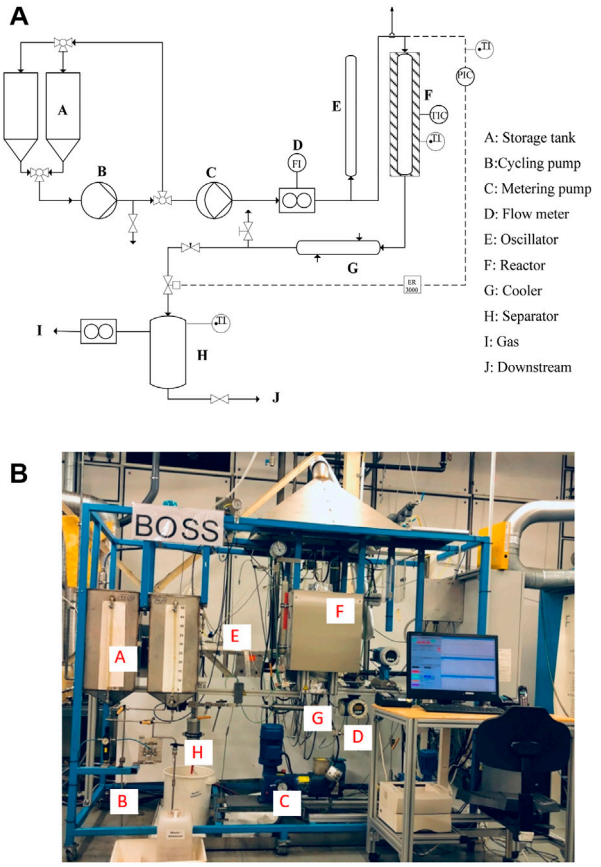

FIGURE 1
(A) piping and instrumentation diagram of the continuously operated plant **(B)** picture of the experimental devices.

The process flow diagram is shown in Figure 1. The system essentially consists of feed tanks with a cycling pump (standard compressed air diaphragm pump from Wilden), a high-pressure metering pump (NOVADOS BRAN LUEBBE NP31, at an approximate pressure up to 250 bar at flow rates of up to 15 L/h); a vertical, plug flow reactor with an internal volume of 350 ml made of 1.4571Ti stainless steel, and product recovery system. The entire plant is controlled *via* WinCC software supplied by Siemens.

For this study, SS feedstock was prepared to ensure a relatively homogeneous paste of ca. 10 wt% solids. 10 wt% (db.) of KOH was added as a homogeneous additive to pre-treat the feed and achieve a better stability of the flow rate (Anastasakis et al., 2018).The flow rates were adjusted to 2 kg/h, leading to residence times within the reactor of around 8 min at a temperature of 350°C. The liquid and solid produced phases that are collected in the separator (H) at a temperature between 50 and 80 °C, were poured in a glass separatory funnel and cooled down to room temperature.

The HTL process was also performed batch-wise in micro-autoclaves with a volume of 24.5 ml, made of stainless steel (1.4571 Ti), which can withstand pressures of up to 40 MPa and a maximum temperature of 400°C. The batch reactors were loaded with pre-weighed samples of SS. Then, the batch reactors were flushed to remove undesired oxygen and then pressurized to 2 MPa using nitrogen gas. Heating was performed in a fluidized sand bath (SBL2, Teche) and kept at the target temperature for the designed reaction time. After the reaction, the reactors were taken out of the heating device and put in cold water to cool down and to stop the reaction. All experiments were executed at least twice to check for reproducibility.

Product separation

Since continuous processing was implemented to study the scale-up of the process, it is believed that a solvent-free procedure is most desirable to collect biocrude that enables industrial application. Phase separation to recover biocrude from the aqueous phase is a challenge as some inorganics may remain in the biocrude phase if gravimetrically collected without any solvents and filtration. Product separation using continuous processing and batch HTL was executed with the procedure described in Figure 2.

The downstream product was poured directly (routine A) to get a mixture including aqueous phase, biocrude and solid residue. The remaining parts in the separatory funnel and autoclaves were rinsed with acetone (routine B) to collect the sticky biocrude and solid residue. The aqueous phase was separated through the addition of a small volume of cyclohexane, which was used as a non-polar solvent to effectively recover the water-insoluble products. And the biocrude was collected using acetone in order to recover the biocrude from solid residues.

Evaporation of the solvent used to recover the biocrude was performed in order to minimize the quantity of volatiles in biocrude, as reported by Prestigiacomo et al. (2020). The controlled evaporation process was performed at 50°C for around 6 h under a continuous flow of N_2 (approximate flow rate of 1 L/min). The produced vapours were condensed in a cold trap cooled at −10°C by a chiller. After evaporation, the biocrude was condensed in the rounded bottom flask, the trapped phase was collected in the glass-jacketed flask.

Product analysis

Biocrude analysis

The C, H, and N contents were measured by the same CHNS-analyser (Vario EL III analysis system, Germany) for solid raw SS samples, with the amount of oxygen content being calculated by difference. The elemental composition was checked for deviations

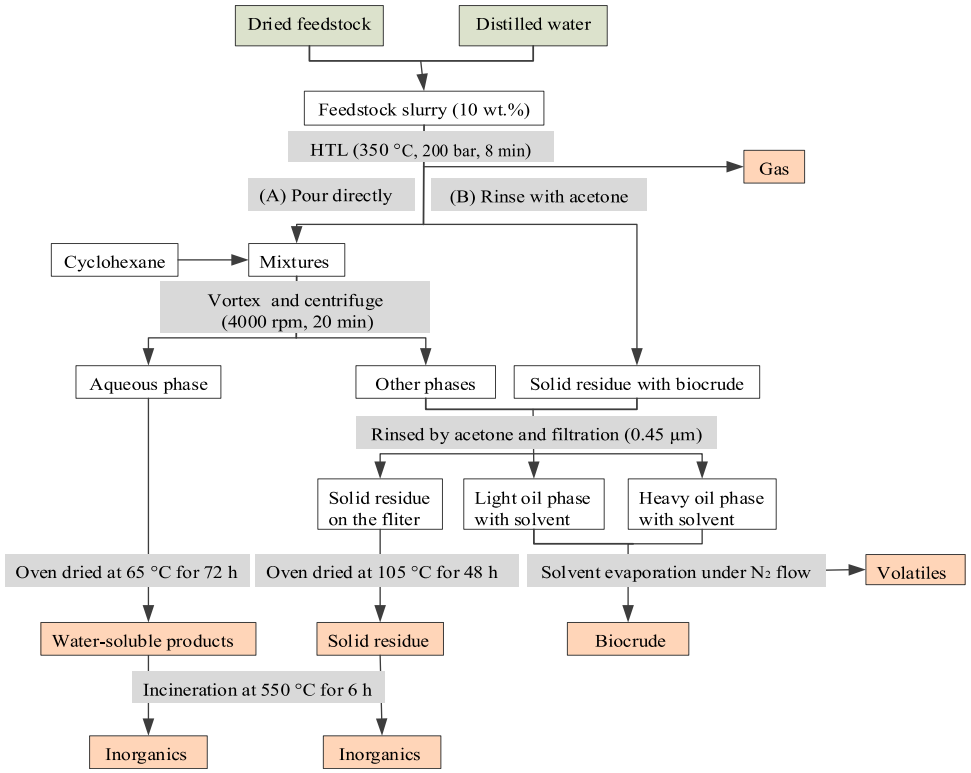

FIGURE 2
Flow chart of procedures for product separation and extraction from continuous and batch HTL process.

by way of 10 measurements of one selected representative biocrude sample. The statistical deviations of C, H, and N were found to be 0.45, 3.03, and 0.69%, respectively (Fan et al., 2020b).

Qualitative analysis of biocrude was carried out using an Agilent 6890N gas chromatograph (GC) with an Agilent 5973 MSD mass spectrometry (MS) detector and a DB-5 capillary column (30 m × 0.25 mm × 0.25 μm) after diluting with THF (1:10 ml/ml) and filtering with a 0.20 μm polytetrafluoroethylene (PTFE) filter. The substances were identified using the NIST library, considering only molecules with an identification probability of more than 80%. The amount of the different compounds was estimated with the relative peak area percentage method.

The quantitative analysis of selected chemicals identified by GC-MS was carried out utilizing two GC-FID devices. Mostly non-polar chemicals were measured by GC-FID with an Agilent DB-5 capillary column (30 m × 0.25 mm × 0.25 μm). The GC oven column temperature was kept at 80°C for 2 min, held at 175°C for 5 min, after ramping at 5 °C/min, and held at 250°C for 8 min after ramping at 30°C/min. Organic acids were analysed by GC-FID with Restek-11023 Stabilwax-DA capillary column (30 m × 0.25 mm × 0.25 μm). The GC oven column temperature was kept at 40°C for 6 min, then increased to 225°C for 0 min at 10°C/min, and held at 250°C for 15 min after ramping at 30°C/min.

Trapped phase analyses

The composition, mainly hydrocarbon fraction, of the trapped liquid phase was also analysed using a Perkin Elmer Autosystem XL GC equipped with a capillary column ZB. FFAP (30 m × 0.25 mm × 0.25 μm). The detection of C10 – C18 hydrocarbon fractions was allowed following a heating of the oven at 40°C for 3 min, then 8°C/min to 244°C for 0 min maintaining 244°C. The injector and the detector were kept at 250°C. The split ratio was 15:1, the He flow-rate in the column was 2.4 ml/min and 0.4 μL was the injection volume.

Aqueous phase analysis

The total carbon (TC), total inorganic carbon (TIC) and total nitrogen (TN) content in the aqueous phase (AQ) were measured with a Dimatec® 2100 instrument. Ammonium (NH_4^+), nitrate (NO_3) and nitrite (NO_2^-) were investigated with a Metrohm 838 advanced sample processor device. Organic acids were analysed with an Aminex HPX-87H column (Biorad, Hercules, CA, United States). The mineral composition in the aqueous phase was analysed using an ICP-OES spectrometer (Agilent Technologies725, Australia) after dissolution in HCl and HNO_3.

Solid residue analysis

The ash content was determined by weight loss due to calcination in a muffle oven under atmospheric conditions at 550°C for 5 h (ASTM-E1755). Metals in SS and solid residue using an ICP-OES Spectrometer (Agilent Technologies 725, Australia) after dissolution in 5 ml conc. 37% hydrochloric acid (HCl) and 2 ml conc. 65% nitric acid (HNO_3).

Compared to continuous operation, additional uncertainties occur in the batch experiments due to incomplete recovery as remaining products stick to the micro-autoclave walls after the reaction, and due to the loss of volatile compounds (during extraction solvent removal), water formation, and experimental errors. To confirm the reproducibility and comparability of results, all experiments were carried out in duplicate. In cases where the relative deviation between the two data points was above 10%, the experiment was repeated. In the results, the average values of the data are given.

The product yields (Yi) were calculated in two cases: one is the weight of the recovered mass M_i to the initial total mass of the feedstock M_{feed}, see Eq. 1 as Y^a; the other is the weight of the recovered mass of organic matter (dry ash free-daf) in the product $M_{i\ (daf)}$ related to the total mass of organic matter in the feedstock ($M_{feed\ (daf)}$.), see Eq. 2 as Y^b.

$$Y_i^a\,(wt\ \%) = \frac{M_i}{M_{feed}} \times 100 \tag{1}$$

$$Y_i^b\,(wt\ \%) = \frac{M_{i\,(daf)}}{M_{feed\,(daf)}} \times 100 \tag{2}$$

The elemental distribution is defined as the amount of an element in the product (m_{Ei}) relative to the amount in the SS (m_{Ef}), see Eq. 3.

$$Elemental\ Distribution\ \ (wt\ \%) = \frac{m_{Ei}}{m_{Ef}} \times 100 \tag{3}$$

The higher heating value (HHV; MJ/kg) was estimated using the modified Dulong's formula as given in Eq. 4.

$$HHV\,(MJ/kg) = 0.0338 \times C + 1.428\,(H - O/8) \tag{4}$$

Results

Characterization of sewage sludge

The properties of sludges used in this work are shown in Table 1. The ash content of 24.66 wt% is much lower than in the digested sludge (38.61 wt%) used in previous work (Fan et al., 2020a), but higher than in the mixed SS (10 wt% in the mixture of primary sludge and activated sludge) (Yokoyama et al., 1987). Lower amounts of inorganic material can be beneficial for a continuous plant to run for a longer time without any problem. Relatively higher C and H contents lead to a higher HHV with a value of 17.22 MJ/kg.

Mass balance in continuous operation

The results obtained from processing SS in the continuous reactor are presented in Table 2. In order to achieve homogeneous downstream products, the products were collected after 30 min of continuous processing. The mass balance of pumped feedstock was calculated with the flow rate of 2 kg/h. The product yields are based on the dry-ash free basis. It is noted that the gas yield and composition was not analysed in this work.

Table 2 shows that around 82 wt% mass can be recovered after HTL. As a consequence of the low slurry content in the feedstock (10 wt%), the lowest solid residue (1.9 wt%) is formed after HTL. Regarding the yields of different products, in the dry ash-free basis, biocrude is the main product with 30.84 wt%, followed by the aqueous phase with 17.32 wt%. However, the total organic mass balance only achieves to 54.13 wt%. The missing mass dues to the uncovered gas and loss during solvent evaporation system. In the work here in, a controlled evaporation of the solvents was performed with the same methodologies adopted by Prestigiacomo et al. (Prestigiacomo et al., 2020). At the end of this controlled evaporation a liquid phase is collected in a cold trap and GC-FID analyses were conducted to check the quantity of organic compounds lost during the evaporation of the solvent. The detection of a hydrocarbon fraction (C16 and C18 alkenes) allowed to improve the mass balance closure of the 3.7 wt% dry-ash free basis).

Furthermore, a C and N balance in the produced phases was evaluated in order to characterize the distribution of C and N present in the feedstocks. Table 3 shows that a majority of carbon is converted into the biocrude phase, reaching 42.83 wt%, followed by the aqueous phase, and then into solid residue. In the continuously operating plant, as the gas phase composition was not analysed, it was not possible to determine the carbon loss in the form of gas was not analysed. The majority of feedstock is desired to be converted into biocrude in order to increase its yield and the overall carbon efficiency of the process. Some unrecovered carbon leads to the relatively low (around 81.69%) closure of the carbon balance. However, it is still comparable with other work. Anastasakis et al. (2018) only took account of the aqueous and biocrude phases, which, on average, amounted to 30.6 wt% and 34.8 wt% of the C in the original SS partitioned to the biocrude and processed water, respectively, after continuous flow HTL. Marrone et al. (2018) found that during continuous flow HTL of mixed SS, approximately 60 wt% and 40 wt% of the C was present in the biocrude, respectively, while 20 wt% and 40 wt% of the C was retained in the process water. As result, a cumulative C balance of 94 % and 97%, were achieved respectively.

TABLE 1 Characterization of SS sample.

Moisture (wt%)	Ash (wt%)[a]	Elemental compositions (wt%)[a]					HHV			
		C	H	O[b]	N	S	(MJ/kg)			
75.42	24.66	39.11	5.83	24.51	5.29	0.6	17.22			
Inorganic content (wt%)[a]										
Al	Ca	Fe	Mg	Mn	P	Zn	Ba	K	Na	Cu
0.73	2.53	5.71	0.28	0.06	2.54	0.11	0.04	0.3	0.33	0.02

[a]Dry basis.
[b]Calculated by difference.

TABLE 2 Mass balance and yields (wt%) of products from continuous process at 350°C with 8 min retention time.

HTL	Biocrude		Solid residue		Aqueous phase		Recovery (%)	
	Y[a]	Y[b]	Y[a]	Y[b]	Y[a]	Y[b]	Y[a]	Y[b]
	2.72	30.84	1.90	5.98	77.52	17.32	81.69	54.13

[a]Based on initial total mass of feedstock.
[b]On dry ash-free basis.

TABLE 3 C and N distribution (CD/ND, wt%) of products from continuous process at 350°C with 8 min retention time.

Biocrude		Solid residue	Aqueous phase	Recovery (%)
CD	42.83	7.71	30.93	81.69
ND	17.13	2.94	51.34	71.42

The outcomes from the literature demonstrated that an optimization of the operative parameters in a continuously operated HTL plant can improve the C recovery to the biocrude. Suggestable temperature for HTL can be designed higher than 300°C, with the retention time less than 30 min. The majority of N is distributed into the aqueous phase, around half is converted, such as water-soluble N-containing products, ammonium and nitrate (Supplementary Table S1), almost three times higher than that partitioned into the biocrude phase. Only 2.93 wt% remains in the solid residue. Quite interestingly, the recovery of N is 10% lower than that of C across the products. The "missing" N was probably lost in the form of volatiles during the evaporation of solvents and drying the solid residues.

Biocrude characterization

The biocrude produced from the continuously operated plant was characterized by a 72.1 wt% C, 9.9 wt% H, 3.9 wt% N, 0.8 wt % S, and the O content, by difference, was 13.3 wt%. The HHV was 36.3 MJ/kg.

The semi-quantitative results for the molecular compositions of biocrude analysed by GC-MS are listed in Table 4. The chemical compounds detected can be divided into five functional groups. O-containing compounds formed majority of compounds identified in the biocrude, mainly phenolic compounds, acids and ketones. This is consistent with the high O content of the obtained biocrude. These oxygenated aromatic or cyclic molecules may be ascribed to the carbohydrates and lignin content in SS. From the literature on HTL of lignin, it can be observed that six carbon-containing compounds (phenols, guaiacols and benzene) are mainly originated from the depolymerization of the lignin component under subcritical and supercritical conditions. Furthermore, five other O-containing oxygenates, including cyclopentanones, furfurals, and cyclopentenones, were derived from carbohydrates (Chumpoo and Prasassarakich, 2010; Carrier et al., 2012). Aliphatic acids like tetradecenoic acid were a product of lipid hydrolysis. Other types of compounds were derived from the lipids, mostly in the form of long-chain aliphatic molecules and cyclic hydrocarbons, including the major compounds in biocrude, which are hexadecane (5.4%), cyclohexadecane (2.7%), and cyclotetradecane (2.6%), indicating that decarboxylation occurred in the HTL process.

Certain amounts of nitrogenous compounds from the continuously operated plant were also found in the biocrude. Specifically speaking, they may be derived from the decarboxylation and rearrangement of amino acids. N-containing heterocycles such as indoles and pyridines are generally generated as a

10.3389/fenvs.2022.996353

TABLE 4 Identified main components with relative area percentage in the total ion chromatogram of biocrude obtained from continuous flow HTL of SS at 350°C with 8 min RT (retention time).

RT	Components	Formula	(%)
	N-heterocycles		
29.77	1-Azetidinecarboxaldehyde, 2,2,4,4-tetramethyl-	$C_8H_{15}NO$	1.7
46.97	Quinoline, 4-methyl-	$C_{10}H_9N$	1.0
47.47	1H-Indole, 4-methyl-	C_9H_9N	3.2
51.10	Pyridine, 3-phenyl-	$C_{11}H_9N$	3.6
74.02	9H-Pyrido [3,4-b]indole, 1-methyl-	$C_{12}H_{10}N_2$	1.1
74.78	1H-Naphth [1,2-d]imidazole	$C_{11}H_8N_2$	1.2
71.50	1-Cyclohexyliminomethyl-naphthalen-2-ol	$C_{17}H_{19}NO$	0.9
	Amides and amines		
32.36	2,2,6,6-Tetramethyl-4-piperidone	$C_9H_{17}NO$	1.4
55.02	(3-Methoxy-2-nitrophenyl)acetic acid, methyl ester	$C_{10}H_{11}NO_5$	1.2
72.59	Tetradecanamide	$C_{14}H_{29}NO$	1.1
	O-containing compounds		
13.79	3-Penten-2-one, 4-methyl-	$C_6H_{10}O$	3.2
16.07	2-Pentanone, 4-hydroxy-4-methyl-	$C_6H_{12}O_2$	5.0
20.34	Butyrolactone	$C_4H_6O_2$	1.5
31.29	Phenol, 4-methyl-	C_7H_8O	3.3
36.15	Phenol, 4-ethyl-	$C_8H_{10}O$	2.5
41.21	Phenol, 4-ethyl-2-methoxy-	$C_9H_{12}O_2$	2.7
45.79	Phenol, 2-methoxy-4-propyl-	$C_{10}H_{14}O_2$	2.1
49.79	Bicyclo [3.3.0]oct-2-en-8-one, 3-methyl-	$C_9H_{12}O$	2.2
50.12	Phenol, 2-methoxy-4-(1-propenyl)-, (E)-eugenol	$C_{10}H_{12}O_2$	2.0
50.51	3-tert-Butyl-4-hydroxyanisole	$C_{11}H_{16}O_2$	2.3
55.71	1-(4-Methoxymethyl-2,6-dimethylphenyl)ethanol	$C_{12}H_{18}O_2$	2.0
56.84	Benzene, 2-(1,1-dimethylethyl)-1,4-dimethoxy-	$C_{12}H_{18}O_2$	1.6
58.77	Benzophenone	$C_{13}H_{10}O$	2.0
61.02	2-Pentadecanone	$C_{15}H_{30}O$	1.0
64.79	Cyclobutanecarboxylic acid, 2-methyloct-5-yn-4-yl ester	$C_{14}H_{22}O$	2.5
69.43	9-Tetradecenal, (Z)-	$C_{14}H_{26}O$	0.9
72.06	Z-7-Tetradecenoic acid	$C_{14}H_{26}O_2$	1.9
75.91	Z-6-Tetradecen-1-ol acetate	$C_{14}H_{26}$	3.5
	Hydrocarbons		
51.72	1-Tridecene	$C_{13}H_{36}$	1.5
53.33	Benzene, 1-methyl-2-(phenylmethyl)-	$C_{14}H_{14}$	1.9
54.66	2-Tetradecene, (E)-	$C_{14}H_{28}$	2.4
60.19	Cyclotetradecane	$C_{14}H_{28}$	2.6
60.74	Cyclopentadecane	$C_{15}H_{30}$	1.1
62.28	9H-Fluorene, 9,9-dimethyl-	$C_{15}H_{14}$	1.1
67.89	Z-1,6-Tridecadiene	$C_{13}H_{24}$	2.6
68.68	1-Hexadecene	$C_{16}H_{32}$	5.4
76.81	Cyclohexadecane, 1,2-diethyl-	$C_{20}H_{40}$	2.7

result of Maillard reactions. Long-chain saturated tetradecanamide was detected, probably originating from the amidation between lipids and proteins (Fan et al., 2020b).

The more volatile components in the biocrude might evaporate during solvent removal. As described above, these components were cold-trapped with the stripped off solvent. The analysis of the trapped components by GC-MS is shown in Figure 3. Several peaks can be detected before the retention time of 25 min. These chemicals with carbon numbers of less than 8, as listed in Table 5, consist to 30.7% of 1-Methoxy-1-propene, and 21.2%

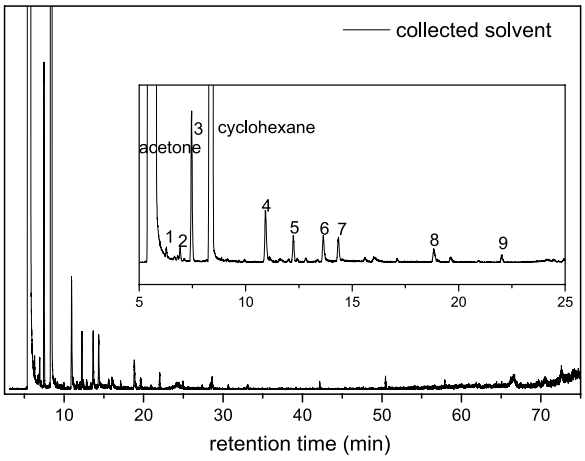

FIGURE 3
GC-MS total ion chromatograms of volatiles obtained from solvent removal after biocrude extraction.

TABLE 5 Identified main components with relative area percentage in the total ion chromatogram of volatiles in the solvent collected from continuous flow HTL of SS at 350°C with 8 min RT (retention time).

Number	RT	Chemicals	Formula	(%)
1	6.28	3-Hexanamine	$C_6H_{15}N$	1.93
2	6.93	Furan, 2-methyl-	C_5H_6O	2.57
3	7.47	1-Methoxy-1-propene	C_4H_8O	30.77
4	10.93	1H-Pyrrole, 1-methyl-	C_5H_7N	13.25
5	12.24	Toluene	C_7H_8	6.39
6	13.65	3-Hexen-2-one	$C_6H_{10}O$	6.19
7	14.36	1H-Pyrrole, 1-ethyl-	C_6H_9N	5.96
8	18.83	Bicyclo [4.2.0]octa-1,3,5-triene	C_8H_8	3.94
9	22.04	1H-Pyrrole, 1-butyl-	$C_8H_{13}N$	2.01

of pyrroles. This is in accordance with the report from Wu et al. (Wu et al., 2017), some N-containing hydrocarbons (C6-C9) with relatively low molecular weights are present in the biocrude from SS. Such a high number of pyrroles as found in the trapped phase can probably be explained by the relatively low N content observed in the acetone-extracted biocrude. In addition, 1.93% hexanamine is found in the trapped phase.

Comparison between continuous and batch HTL

This section provides a comparison between the performance of batch and continuous flow HTL. The batch experiments were conducted at the same continuous processing conditions.

The product yields for batch and continuous experiments are shown in Figure 4. The total mass balance of condensed products shown in Figure 4A displays a better mass closure obtained for continuous flow HTL, reaching 81.7 wt% compared to 76.2 wt% and 81.6 wt% achieved with batch HTL of SS without and with KOH, respectively. This observation is probably due to the higher volume of feedstocks processed during continuous flow HTL, which can reduce the impact of missing materials during the collection and separation procedures. In both types of experiments, the aqueous phase is the major product after HTL, and, owing to the initial feedstock concentration, 90 wt % is water. Regarding the yields of organic products as shown in Figure 4B, biocrude is the dominant product with around 30 wt%.

In the case of catalytic batch HTL, KOH has a slight effect on the biocrude yields, which is in line with other work (Malins et al., 2015; Shah et al., 2020). The alkali catalyst has negligible effects on the yields of biocrude from HTL of SS, while, the gases yields were largely decreased, owing to the capture of CO_2 (Supplementary Table S3). However, as can be seen, the presence of KOH dramatically suppresses the formation of char leading to lower yields of solid residue, and catalyses the conversion of water-soluble organics.

Batch and continuous HTL processes also exhibit differences in the quality of the produced biocrude in terms of its elemental composition (Table 6). In the presence of KOH, the C, H and N contents are higher in batch operation, while the O and S contents are higher in the continuous process.

The organic compounds in the biocrude were identified by GC-MS, with the component fractions shown in Figure 5. The comparison of total ion chromatograms was shown in Supplementary Figure S1. No significantly differences were found in the type of molecules detected by GC-MS in the biocrude from batch processing in the presence or absence of KOH. It was observed that some more N-containing heterocycles were produced with the addition of KOH. Compared with continuously operated HTL plant, several different peaks can be observed, as marked by the numbers and listed in Table 7. The various peaks observed in the total ion chromatogram evidently indicate that a faster heating rate improves the formation of oxygenates, as suggested by the higher O content found in the biocrude from continuous flow HTL.

(Z)-9-Octadecenamide was found in the biocrude from batch processing, being a long-chain aliphatic amide, accounting for 10.2 and 7.5 wt% in the bio-crude from the top 50 peaks identified, hence resulting in higher amides.

The carbon and nitrogen distribution cross the products are compared in Table 8. As a general trend, it can be seen the majority of C is converted into the biocrude phase, less than one third of C is recovered in aqueous products. In contrast to this, half of N is transformed into the aqueous phase, while less than one sixth remains in the solid residue (0.8 wt% N in the solid residue, seen Supplementary Table S2), and more than half of N is obtained with a significant proportion of ammonium (27.6–30.9 wt%). Only a trace amount (<40 mg/L) of nitrate is

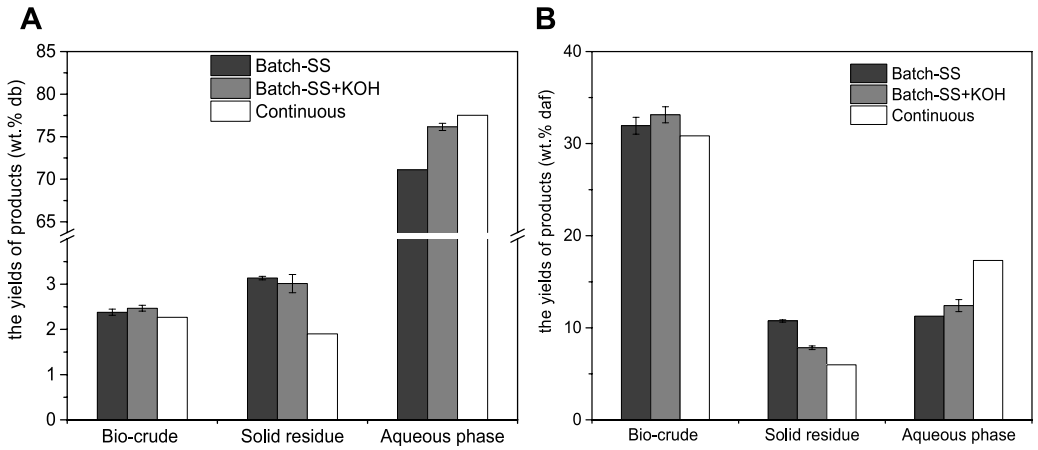

FIGURE 4
Comparison of product yields from batch and continuous flow HTL experiments with an SS loading of 10 wt% at 350°C with 8 min retention time, **(A)** on dry basis; **(B)** on dry-ash free basis.

TABLE 6 Comparison of elemental composition and higher heating values in the biocrude obtained from batch and continuous HTL of sludge at 350°C with 8 min retention time.

Samples	Elemental content (wt%)[a]					HHV
	C	H	Ob	N	S	(MJ/kg)
Batch-SS	72.24	10.04	12.32	4.76	0.64	36.71
Batch-SS + KOH	72.98	10.51	11.66	4.25	0.60	37.76
Continuous	72.10	9.90	13.30	3.90	0.80	36.28

[a]On a dry basis.
[b]Calculated by difference.

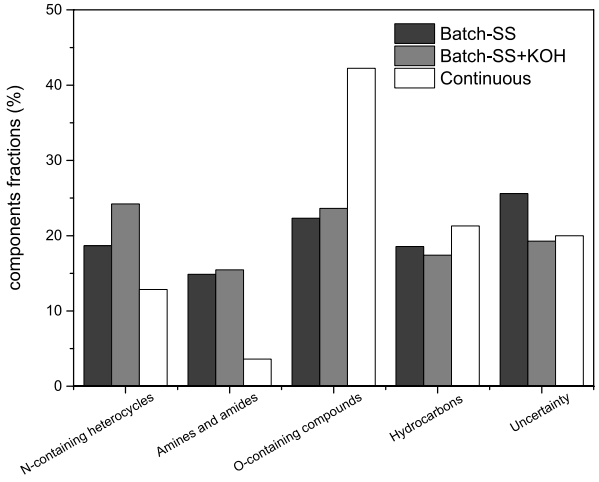

FIGURE 5
Comparison of component fractions in biocrude obtained from batch and continuous flow HTL of sewage sludge at a concentration of 10 wt% under 350°C with 8 min retention time.

found in the products of batch HTL of SS, and the presence of other organic nitrogen-containing molecules in the aqueous product is clearly indicated by the gap between total nitrogen and nitrogen in the form of ammonium, respectively, in the range of 20.5–22.9 wt%.

Discussion

The biocrude obtained in this work is much lower than the findings of Itoh et al. (1992), who obtained 40–53 wt% of heavy oil with a continuous process. That can be explained with the employed separation procedure, because they used DCM as solvent to extract the biocrude from the other produced phases. In the study herein, the effects of DCM in the yields of biocrude were verified, selected experiments were conducted placing DCM in the place of cyclohexane to the aqueous phase. It is observed that an average of 18.2 wt% organic content in the aqueous phase can be extracted using DCM. If this organic fraction is considered as additional mass to the collected biocrude, at least 3.1 wt% can be added to its yield. On the other hand, the yield obtained in this work is higher than that reported by Aarhus University (Anastasakis et al., 2018), mostly due to the lower initial slurry concentration (4 wt%) and the solvent-free separation of biocrude used in their work. The use of organic solvents for the separation of biocrude in batch systems can result in the extraction of additional organics from the water phase and/or the solids leading to an increase in the

TABLE 7 The different components identified by GC-MS of the biocrude from continuous flow HTL of SS at 350°C with 8 min RT (retention time).

Number	RT	Chemicals	Formula
1	13.8	3-Penten-2-one, 4-methyl-	$C_6H_{10}O$
2	32.4	2,2,6,6-Tetramethyl-4-piperidone	$C_9H_{17}NO$
3	38.8	Unknown	
4	41.2	Phenol, 4-ethyl-2-methoxy-	$C_9H_{12}O_2$
5	49.8	Bicyclo [3.3.0]oct-2-en-8-one, 3-methyl-	$C_9H_{12}O$
6	50.1	Phenol, 2-methoxy-4-(1-propenyl)-, (E)-	$C_{10}H_{12}O_2$
7	64.8	Cyclobutanecarboxylic acid, 2-methyloct-5-yn-4-yl ester	$C_{14}H_{22}O$
8	73.5	(Z)-9-Octadecenamide	$C_{18}H_{35}NO$

TABLE 8 Comparison of elemental distributions (wt%) across various products from batch and continuous HTL of sludge at 350°C with 8 min RT (retention time).

Samples	Bio-crude		Solid residue		Aqueous phase		Recovery	
	CD	ND	CD	ND	CD	ND	CD	ND
Batch-SS	45.76	22.40	14.26	9.63	23.66	50.51	83.68	82.55
Batch-SS + KOH	47.94	20.72	11.06	5.46	30.74	61.01	89.74	87.19
Continuous	42.83	17.13	7.71	2.94	30.93	51.34	81.47	71.41

measured biocrude yields (Watson et al., 2019). The recovery of organic contents is observed half around. This can be explained by the uncertainty due to the missing gas, mass not detected during the separation and the sampling procedures, and evaporation of volatiles during the drying and solvent evaporation process (Li et al., 2021). During the separation procedures adopted coherently with the literature, when an organic solvent was adopted to recover the biocrude, a step of evaporation of the solvent is always needed to collect biocrude mass. Most of the time during this evaporation procedures, a fraction of organic compounds collected with biocrude can be stripped away with solvents and they were represented missing matter.

The reduction of the N and O content in the biocrude indicates that the removal of heteroatoms is enhanced during continuous flow HTL, mostly because of the typical reactions occurring in hydrothermal conditions such as decarboxylation, dehydration and deamination (Pongsiriyakul et al., 2021). The C content is very comparable to what was reported by Marrone et al. (2018), 76.5 wt% and 72.8 wt% were found in the biocrude produced by HTL of primary and secondary SS, respectively. Regarding the values of N content about 4.3 and 5.1 wt%, it should be said that, in the work herein, the lower N content is probably due to the relatively lower N content in the native SS.

Comparing continuous and batch processes, the biocrude obtained through batch processing shows higher yields than in continuous flow HTL, which is unexpected, because a faster heating rate was supposed to enhance biocrude production (Akhtar and Amin, 2011; Faeth et al., 2013). In this case, this can possibly be explained by the different collection procedure. One more step was applied in the batch reactor: the inner wall of the reactor was washed with solvent, leading to the collection of the stickier biocrude than in continuous flow HTL. Moreover, comparable results were also reported from HTL of microalgae. Barreiro et al. (2015) investigated the difference in biochemical fractions of feedstock and the orders of HTL reaction kinetics. Many molecules involved in the HTL process show a different reactivity. The repolymerization of water-soluble intermediates that form biocrude or char normally exhibits reaction orders higher than one (Chuntanapum and Matsumura, 2009; Wang et al., 2020). In a continuous tube reactor, the decrease of biocrude yield with an increase in water-soluble products indicates that the rate of the pathways with reaction orders higher than one was reduced. Therefore, the choice of a batch or continuous reactor will influence the concentration of the various molecules in the reaction medium, thus affecting the reaction kinetics and the final product yields of the HTL process.

The higher N content in batch reactions is probably caused by the higher relevance of N-heterpcyclic formation reactions occurring in batch systems during the heating transient and cooling period. Phenomena that can be more relevant in the batch procedures respect to the plug flow reactor of the

continuous plant. The pathways toward the formation of biocrude from proteins typically imply the occurrence of repolymerization reactions (Chuntanapum and Matsumura, 2009). After certain holding time, the intermediates may behave unstable, leading to the N-formation by chelation or repolymerization in cooling period. As depicted inTable 1, the components identified in trapped phase mainly consist of some pyrrole derivatives, which may further chelate and aggregate into macromolecules remain into oily phase.

In addition, they can be ascribed to Maillard reactions and amidation reaction, which can generate N-containing heterocycles during the heating-up period (Fan et al., 2018). Maillard reactions can occur between reducing carbohydrates and active amino acids at low temperatures of about 150°C, which means the melanoidin-like products can be generated at lower temperatures. In the present study, even when a faster heating rate (36 C/min) than in batch processing was applied, it still took a while to reach 350°C.

The observation of a higher O content in the biocrude from continuous HTL is in line with the reports of fast HTL of SS (Qian et al., 2017), indicating that an increase in the heating rate inhibits the degradation or increases the formation of oxygenates. Theoretically, either the reaction rate of decarboxylation or the dehydration is reduced. The further analysis of CO_2 in the gases from continuous HTL might help to explain this. The addition of KOH shows an increase in C and H with a decrease in O, N and S content, therefore leading to the highest heating values.

The addition of KOH improves water-soluble products, especially the recovery of N is greatly increased from 50 to 60 wt%. Therefore, it becomes necessary to design efficient routes to implement water management in HTL processes. Increasing attention is paid to the recovery of organics and nutrients from the aqueous stream (Biller et al., 2012; Leng et al., 2021), as well as to energy recovery (Yang et al., 2018; Si et al., 2019).

Conclusion

HTL experiments with continuous flow processing were successfully conducted for SS in the presence of KOH at 350°C, 200 bar and a retention time of 8 min. Without the collection of gases, 88 wt% mass balance can be achieved. 30.8 wt% biocrude was obtained, which is, however, slightly lower than in batch processing, probably because the repolymerization of water-soluble products to form biocrude was reduced. The type of chemical components in the biocrude from both processes identified by GC-MS is similar. No significant effects were found in terms of the yields of biocrude from continuous flow HTL while applying instant heating rates to achieve the reaction temperature. However, it was observed that the continuously operated HTL plant leads to obtain a biocrude with a lower content of N with respect to the batch operated HTL adopting similar operative condition. The higher N content found after batch processing can be due to the significant effects of Maillard reactions and amidation that occur during the heating up period, and the N-formation of unstable intermediates during cooling down stage. In any case, comparing batch and continuous flow HTL is a complex subject because of the difficulty in accounting for the effect of the heating and cooling periods, even though the same separation procedure is applied.

Data availability statement

The datasets presented in this study can be found in online repositories. The names of the repository/repositories and accession number(s) can be found in the article/ Supplementary Material.

Author contributions

YF: Conceptualization, Methodology, Investigation, Visualization Writing original draft. CP: Conceptualization, Methodology, Investigation. TT: Conceptualization, Methodology, Investigation. MG: Investigation, Visualization. UH: Conceptualization, Project administration, Supervision. ND: Investigation, Supervision, Writing review and editing.

Funding

The authors gratefully acknowledge the financial support from the National Natural Science Foundation (52000056) of PR China, the Science and Technology Research Project in Henan Province (222102520029) the Start-up Foundation of Nanyang Institute of Technology, China (510162) and the Ecological Environment and Resources Research Center of Nanyang Institute of Technology.

Acknowledgments

Armin Lautenbach, Birgit Rolli, Alexandra Böhm, Jessica Mayer, and Sonja Habicht are thanked gratefully for their skillful technical assistance.

Conflict of interest

The authors declare that the research was conducted in the absence of any commercial or financial

relationships that could be construed as a potential conflict of interest.

Publisher's note

All claims expressed in this article are solely those of the authors and do not necessarily represent those of their affiliated organizations, or those of the publisher, the editors and the reviewers. Any product that may be evaluated in this article, or claim that may be made by its manufacturer, is not guaranteed or endorsed by the publisher.

Supplementary Material

The Supplementary Material for this article can be found online at: https://www.frontiersin.org/articles/10.3389/fenvs.2022.996353/full#supplementary-material

References

Akhtar, J., and Amin, N. A. S. (2011). A review on process conditions for optimum bio-oil yield in hydrothermal liquefaction of biomass. *Renew. Sustain. Energy Rev.* 15, 1615–1624. doi:10.1016/j.rser.2010.11.054

Ali Shah, A., Sohail Toor, S., Hussain Seehar, T., Sadetmahaleh, K. K., Helmer Pedersen, T., Haaning Nielsen, A., et al. (2021). Bio-crude production through co-hydrothermal processing of swine manure with sewage sludge to enhance pumpability. *Fuel* 288, 119407. doi:10.1016/j.fuel.2020.119407

Anastasakis, K., Biller, P., Madsen, R., Glasius, M., and Johannsen, I. (2018). Continuous hydrothermal liquefaction of biomass in a novel pilot plant with heat recovery and hydraulic oscillation. *Energies* 11, 2695. doi:10.3390/en11102695

Barreiro, D. L., Gómez, B. R., Hornung, U., Kruse, A., and Prins, W. (2015). Hydrothermal liquefaction of microalgae in a continuous stirred-tank reactor. *Energy* 29, 6422–6432. doi:10.1021/acs.energyfuels.5b02099

Biller, P., Ross, A. B., Skill, S. C., Lea-Langton, A., Balasundaram, B., Hall, C., et al. (2012). Nutrient recycling of aqueous phase for microalgae cultivation from the hydrothermal liquefaction process. *Algal Res.* 1, 70–76. doi:10.1016/j.algal.2012.02.002

Carrier, M., Loppinet-Serani, A., Absalon, C., Aymonier, C., and Mench, M. (2012). Degradation pathways of holocellulose, lignin and α-cellulose from Pteris vittata fronds in sub- and super critical conditions. *Biomass Bioenergy* 43, 65–71. doi:10.1016/j.biombioe.2012.03.035

Chumpoo, J., and Prasassarakich, P. (2010). Bio-oil from hydro-liquefaction of bagasse in supercritical ethanol. *Energy* 24, 2071–2077. doi:10.1021/ef901241e

Chuntanapum, A., and Matsumura, Y. (2009). formation of tarry material from 5-HMF in subcritical and supercritical water. *Ind. Eng. Chem. Res.* 48, 9837–9846. doi:10.1021/ie900423g

Djandja, O. S., Yin, L.-X., Wang, Z.-C., and Duan, P.-G. (2021). From wastewater treatment to resources recovery through hydrothermal treatments of municipal sewage sludge: A critical review. *Process Saf. Environ. Prot.* 151, 101–127. doi:10.1016/j.psep.2021.05.006

Elliott, D. C., Biller, P., Ross, A. B., Schmidt, A. J., and Jones, S. B. (2015). Hydrothermal liquefaction of biomass: Developments from batch to continuous process. *Bioresour. Technol.* 178, 147–156. doi:10.1016/j.biortech.2014.09.132

Faeth, J. L., Valdez, P. J., and Savage, P. E. (2013). Fast hydrothermal liquefaction of nannochloropsis sp. to produce biocrude. *Energy* 27, 1391–1398. doi:10.1021/ef301925d

Fan, Y., Fonseca, F. G., Gong, M., Hoffmann, A., Hornung, U., and Dahmen, N. (2020a). Energy valorization of integrating lipid extraction and hydrothermal liquefaction of lipid-extracted sewage sludge. *J. Clean. Prod.* 285, 124895. doi:10.1016/j.jclepro.2020.124895

Fan, Y., Hornung, U., Dahmen, N., and Kruse, A. (2018). Hydrothermal liquefaction of protein-containing biomass: Study of model compounds for maillard reactions. *Biomass Convers. biorefin.* 8, 909–923. doi:10.1007/s13399-018-0340-8

Fan, Y., Hornung, U., Raffelt, K., and Dahmen, N. (2020b). The influence of lipids on the fate of nitrogen during hydrothermal liquefaction of protein-containing biomass. *J. Anal. Appl. Pyrolysis* 147, 104798. doi:10.1016/j.jaap.2020.104798

Gherghel, A., Teodosiu, C., and De Gisi, S. (2019). A review on wastewater sludge valorisation and its challenges in the context of circular economy. *J. Clean. Prod.* 228, 244–263. doi:10.1016/j.jclepro.2019.04.240

He, C., Chen, C.-L., Giannis, A., Yang, Y., and Wang, J.-Y. (2014). Hydrothermal gasification of sewage sludge and model compounds for renewable hydrogen production: A review. *Renew. Sustain. Energy Rev.* 39, 1127–1142. doi:10.1016/j.rser.2014.07.141

He, Y., Liang, X., Jazrawi, C., Montoya, A., Yuen, A., Cole, A. J., et al. (2016). Continuous hydrothermal liquefaction of macroalgae in the presence of organic co-solvents. *Algal Res.* 17, 185–195. doi:10.1016/j.algal.2016.05.010

Huang, H.-J., Chang, Y.-C., Lai, F.-Y., Zhou, C.-F., Pan, Z.-Q., Xiao, X.-F., et al. (2019). Co-liquefaction of sewage sludge and rice straw/wood sawdust: The effect of process parameters on the yields/properties of bio-oil and biochar products. *Energy* 173, 140–150. doi:10.1016/j.energy.2019.02.071

Itoh, S., Suzuki, A., Nakamura, T., and Yokoyama, S.-Y. (1994). Production of heavy oil from sewage sludge by direct thermochemical liquefaction. *Desalination* 98, 127–133. doi:10.1016/0011-9164(94)00137-5

Itoh, S., Suzuki, A., Nakamura, T., and Yokoyama, S. (1992). Direct thermochemical liquefaction of sewage sludge by a continuous plant. *Water Sci. Technol.* 26, 1175–1184. doi:10.2166/wst.1992.0559

Jazrawi, C., Biller, P., Ross, A. B., Montoya, A., Maschmeyer, T., and Haynes, B. S. (2013). Pilot plant testing of continuous hydrothermal liquefaction of microalgae. *Algal Res.* 2, 268–277. doi:10.1016/j.algal.2013.04.006

Jensen, C. U., Rodriguez Guerrero, J. K., Karatzos, S., Olofsson, G., and Iversen, S. B. (2017). Fundamentals of Hydrofaction™: Renewable crude oil from woody biomass. *Biomass Convers. biorefin.* 7, 495–509. doi:10.1007/s13399-017-0248-8

Johannsen, I., Kilsgaard, B., Milkevych, V., and Moore, D. (2021). Design, modelling, and experimental validation of a scalable continuous-flow hydrothermal liquefaction pilot plant. *Process. (Basel).* 9, 234. doi:10.3390/pr9020234

Leng, L., Yang, L., Chen, J., Hu, Y., Li, H., Li, H., et al. (2021). Valorization of the aqueous phase produced from wet and dry thermochemical processing biomass: A review. *J. Clean. Prod.* 294, 126238. doi:10.1016/j.jclepro.2021.126238

Leng, L., Zhang, W., Peng, H., Li, H., Jiang, S., and Huang, H. (2020). Nitrogen in bio-oil produced from hydrothermal liquefaction of biomass: A review. *Chem. Eng. J.* 401, 126030. doi:10.1016/j.cej.2020.126030

Li, S., Jiang, Y., Snowden-Swan, L. J., Askander, J. A., Schmidt, A. J., and Billing, J. M. (2021). Techno-economic uncertainty analysis of wet waste-to-biocrude via hydrothermal liquefaction. *Appl. Energy* 283, 116340. doi:10.1016/j.apenergy.2020.116340

Lin, Y.-Y., Chen, W.-H., and Liu, H.-C. (2020). Aging and emulsification analyses of hydrothermal liquefaction bio-oil derived from sewage sludge and swine leather residue. *J. Clean. Prod.* 266, 122050. doi:10.1016/j.jclepro.2020.122050

Lu, J. L., Dong, G. R., Chen, F., and Wang, J. B. (2016). Research progress of oil making from sewage sludge. *Appl. Mech. Mater.* 851, 232–236. doi:10.4028/www.scientific.net/amm.851.232

Malins, K., Kampars, V., Brinks, J., Neibolte, I., Murnieks, R., and Kampare, R. (2015). Bio-oil from thermo-chemical hydro-liquefaction of wet sewage sludge. *Bioresour. Technol.* 187, 23–29. doi:10.1016/j.biortech.2015.03.093

Marrone, P. A., Elliott, D. C., Billing, J. M., Hallen, R. T., Hart, T. R., Kadota, P., et al. (2018). Bench-scale evaluation of hydrothermal processing technology for conversion of wastewater solids to fuels. *Water Environ. Res.* 90 (4), 329–342. doi:10.2175/106143017X15131012152861

Pongsiriyakul, K., Kiatkittipong, W., Adhikari, S., Lim, J. W., Lam, S. S., Kiatkittipong, K., et al. (2021). Effective Cu/Re promoted Ni-supported γ-Al2O3 catalyst for upgrading algae bio-crude oil produced by hydrothermal liquefaction. *Fuel Process. Technol.* 216, 106670. doi:10.1016/j.fuproc.2020.106670

Prestigiacomo, C., Laudicina, V. A., Siragusa, A., Scialdone, O., and Galia, A. (2020). Hydrothermal liquefaction of waste biomass in stirred reactors: One step forward to the integral valorization of municipal sludge. *Energy* 201, 117606. doi:10.1016/j.energy.2020.117606

Qian, L., Wang, S., and Savage, P. E. (2017). Hydrothermal liquefaction of sewage sludge under isothermal and fast conditions. *Bioresour. Technol.* 232, 27–34. doi:10.1016/j.biortech.2017.02.017

Rahman, T., Jahromi, H., Roy, P., Adhikari, S., Hassani, E., and Oh, T.-S. (2021). Hydrothermal liquefaction of municipal sewage sludge: Effect of red mud catalyst in ethylene and inert ambiences. *Energy Convers. Manag.* 245, 114615. doi:10.1016/j.enconman.2021.114615

Shah, A. A., Toor, S. S., Seehar, T. H., Nielsen, R. S., Nielsen, A. H., Pedersen, T. H., et al. (2020). Bio-crude production through aqueous phase recycling of hydrothermal liquefaction of sewage sludge. *Energies* 13, 493. doi:10.3390/en13020493

Si, B., Yang, L., Zhou, X., Watson, J., Tommaso, G., Chen, W.-T., et al. (2019). Anaerobic conversion of the hydrothermal liquefaction aqueous phase: Fate of organics and intensification with granule activated carbon/ozone pretreatment. *Green Chem.* 21, 1305–1318. doi:10.1039/c8gc02907e

Silva Thomsen, L. B., Carvalho, P. N., Dos Passos, J. S., Anastasakis, K., Bester, K., and Biller, P. (2020). Hydrothermal liquefaction of sewage sludge; energy considerations and fate of micropollutants during pilot scale processing. *Water Res.* 183, 116101. doi:10.1016/j.watres.2020.116101

Wagner, J. L., Le, C. D., Ting, V. P., and Chuck, C. J. (2017). Design and operation of an inexpensive, laboratory-scale, continuous hydrothermal liquefaction reactor for the conversion of microalgae produced during wastewater treatment. *Fuel Process. Technol.* 165, 102–111. doi:10.1016/j.fuproc.2017.05.006

Wang, C., Fan, Y., Hornung, U., Zhu, W., and Dahmen, N. (2020). Char and tar formation during hydrothermal treatment of sewage sludge in subcritical and supercritical water: Effect of organic matter composition and experiments with model compounds. *J. Clean. Prod.* 242, 118586. doi:10.1016/j.jclepro.2019.118586

Watson, J., Lu, J., De Souza, R., Si, B., Zhang, Y., and Liu, Z. (2019). Effects of the extraction solvents in hydrothermal liquefaction processes: Biocrude oil quality and energy conversion efficiency. *Energy* 167, 189–197. doi:10.1016/j.energy.2018.11.003

Wu, S.-Y., Liu, F.-Q., Huang, S., Wu, Y.-Q., and Gao, J.-S. (2017). Direct n-hexane extraction of wet sewage sludge at thermal and pressurized conditions: A preliminary investigation on its process and product characteristics. *Fuel Process. Technol.* 156, 90–97. doi:10.1016/j.fuproc.2016.07.020

Yang, L., Si, B., Tan, X., Chu, H., Zhou, X., Zhang, Y., et al. (2018). Integrated anaerobic digestion and algae cultivation for energy recovery and nutrient supply from post-hydrothermal liquefaction wastewater. *Bioresour. Technol.* 266, 349–356. doi:10.1016/j.biortech.2018.06.083

Yokoyama, S.-Y., Suzuki, A., Murakami, M., Ogi, T., Koguchi, K., and Nakamura, E. (1987). Liquid fuel production from sewage sludge by catalytic conversion using sodium carbonate. *Fuel* 66, 1150–1155. doi:10.1016/0016-2361(87)90315-2

Zimmermann, J., Raffelt, K., and Dahmen, N. (2021). Sequential hydrothermal processing of sewage sludge to produce low nitrogen biocrude. *Processes* 9, 491. doi:10.3390/pr9030491